

ANALYSIS OF THE KALMAN FILTER WITH DIFFERENT INS ERROR MODELS FOR GPS/INS INTEGRATION IN AERIAL REMOTE SENSING APPLICATIONS

Hongxing Sun^a, Jianhong Fu^a, Xiuxiao Yuan^a, Weiming Tang^b

^a School of Remote Sensing & Info. Eng., Wuhan University, P. R. China 430079

^b GNSS Eng. Technology Research Center, Wuhan University, P. R. China 430079

Commission V, ICWG V/I

KEY WORDS: Direct Georeferencing, Aerial Triangulation, GPS/INS Integration, Kalman Filter

ABSTRACT:

In the Kalman filter used for the integration of GPS/INS, the inertial sensor error model is usually considered as a random constant or random walk for both gyroscopes and accelerometers. However, the Inertial Measurement Unit (IMU) used in aerial remote sensing applications for sensor positioning and orientation is typically of tactical grade, i.e., the gyroscope drifts are on the order of 0.1 deg/h and the accelerometer biases are 100ug respectively. In this case, there is the room to improve the system performance by developing more complicated error models for the inertial sensors. In this paper, 6-state, 12-state and 15-state error models for the inertial sensors are implemented, and their performance of each in the Kalman filter is compared and analyzed. Firstly, the commonly used 6-state error model that includes three random walks for gyroscopes and three random walks for accelerometers is implemented. Then, a 12-state error model is formed by augmenting the 6-state model with three scale factors for the gyroscopes and three scale factors for the accelerometers. Thirdly, three first-order Markov procedures are considered for the gyroscopes in addition to the random walks and scale factors, thus resulting in a 15-state error model. Aerial GPS/INS data collected in the field with a tactical grade IMU and dual frequency GPS receivers is processed with these three error models. In the data processing, the loosely-coupled Kalman filter, which is the common coupling method for the aerial GPS/INS integration, is used. The 12-state and 15-state error models show obvious advantages over the 6-state error model in the test results. The accuracies of the integrated position (5cm), velocity (3cm/s) and attitude (0.002 degree for pitch and roll, 0.008 degree for heading) in the 12-state model are all better than that of the 6-state error model. However, the improvement of the 15-state error model relative to the 12-state error model is limited and insignificant.

1. INTRODUCTION

Direct georeferencing, also referred to as direct platform orientation (DPO), is defined as direct measurement of the imaging sensor external orientation parameters (EOP), using positioning and orientation sensors, typically the Global Positioning System (GPS) and Inertial Navigation System (INS) or Inertial Measurement Unit (IMU). With the increasing use of multi-sensor mapping, the DPO of the integrated GPS/IMU systems has become a crucial component of spatial data processing algorithms, and substantial research effort has been devoted to extensive algorithmic developments, performance analysis and practical implementations of GPS/IMU systems (Skaloud *et al.*, 1996; Abdullah, 1997; Grejner-Brzezinska, 1997; Toth and Grejner-Brzezinska, 1998; Grejner-Brzezinska, 1999; Grejner-Brzezinska, 2001; Mostafa *et al.*, 2001; Cramer *et al.*, 2000; Cramer, 2001). However, investigation of the GPS/INS integration itself, especially for the inertial sensor error model, is not focused on as much. Grejner-Brzezinska *et al.*, (2005) attempted to improve the performance of GPS/IMU integration by using a precise gravity model, signal de-noising and parameter refinement of the inertial sensor stochastic model, nevertheless the sensor stochastic model was still of 12 states.

The commonly used IMU sensor stochastic model in the Kalman Filter (KF) supports 6 states (i.e., gyroscope drift and accelerometer bias) to 12 states (for which the scale factors of both of gyroscope and accelerometer are also included) (Cramer, 2001; Grejner-Brzezinska *et al.*, 2005). In aerial photogrammetric mapping or remote sensing, the IMU hardware is typically classified as high-end tactical grade sensor, i.e., the gyroscope drifts are on the order of 0.1 deg/h and the accelerometer biases are 100ug respectively. In this case, there

is the room to improve the system performance by developing more complicated error models for the inertial sensors. In this paper, the 6-state, 12-state and 15-state inertial sensor error models are implemented, and the KF performance of each is compared and analyzed.

2. STOCHASTIC ERROR MODEL OF THE INERTIAL SENEORS

The performance characteristic of a gyroscope (or accelerometer) is determined by the dynamic model, which involves a scale factor, bias and random, random environmental sensitivity and misalignment (IEEE std. 952-1997). The situation is similar for accelerometers (IEEE std. 1293-1998). The environmental sensitivity and misalignment are generally ignored in the stochastic error model, so the focus in this paper is mainly on the first two items. The scale factor of the sensor is calibrated by the manufacturers in the factory before the sale. But post-factory calibration of the instrument can still influence the navigation performance significantly, therefore it can also be considered in the stochastic error model. The random component of the gyroscope and accelerometer data mainly include: (a) the gyro rate ramp (trend) defined as a gyro behavior characterized by quadratic growth within a certain range of time, (b) gyro rate (acceleration) random walk due to white noise in the angular acceleration (jerk) which is defined as the drift rate error (acceleration) build-up with time, (c) flicker noise (bias instability), defined as a random variation in bias, computed over a specific finite sample time and averaging time interval; (d) angle (velocity) random walk due to the white noise of gyroscope angular rate (acceleration) data, (e) quantization noise, defined as a random variation in the digitized output

signal due to sampling and quantizing of a continuous signal with a finite word length conversion, (f) exponentially correlated (Markov) noise characterized by an exponential decaying function with a finite correlation time, and (g) sinusoidal noise characterized by one or more distinct frequencies (IEEE Std. 952–1997 and IEEE Std. 528–2001). Generally, any combination of these processes can be present in the data, and different noise terms may appear in different regions of the time scale. In practical applications, the random items above can be chosen selectively to establish the stochastic error model. From the simplest scenario that only considered bias instability (e. g. see Schwarz, *et al.*, 1994) to moderately complicated models that were augmented with scale factors and axis misalignments (Grejner-Brzezinska, 2001; Cramer, 2001) were used for the aerial photogrammetric applications. In this paper, the random item for the bias in the gyroscope can be considered as:

$$d = d_b + d_R + d_m + w_d \quad (1)$$

Where d denotes random bias, d_b denotes bias instability, d_R denotes gyro rate random walk, d_m denotes first-order Markov process noise, w_d denotes white noise that drives into the angle random walk. A more detailed representation of Equation (1) can be found in (Yi, 2007). The rates of d_b , d_R and d_m are expressed in Equation (2), (3) and (4) as:

$$\dot{d}_b = 0 \quad (2)$$

$$\dot{d}_R = w_{dR} \quad (3)$$

$$\dot{d}_m = -\frac{1}{\alpha} d_m + w_{dm} \quad (4)$$

Where w_{dR} denotes white noise, α denotes the correlation time of the process, w_{dm} denotes white noise. The random item for the bias in the accelerometer can be written as:

$$b = b_b + b_R + b_m + w_b \quad (5)$$

Where the meanings of the suffixes are the same as those in Equation (1), and the rates of b_b , b_R and b_m are expressed in Equation (6), (7) and (8) as:

$$\dot{b}_b = 0 \quad (6)$$

$$\dot{b}_R = w_{bR} \quad (7)$$

$$\dot{b}_m = -\frac{1}{\beta} b_m + w_{bm} \quad (8)$$

Where w_{bR} denotes white noise, β denotes the correlation time of the process, w_{bm} denotes white noise. By ignoring d_R , d_m , b_R and b_m and consideration of only random constants (d_b and b_b), the 6-state error model can be

implemented in the KF. Inclusion of the navigation parameters and other constant parameters (for example, the lever arm of the GPS antenna relative to the INS navigation center) results in the linearized error dynamic equation of the KF given as a state-vector-based linear differential Equation (9):

$$\begin{bmatrix} \dot{x}_{rv\epsilon} \\ \dot{x}_f \\ \dot{x}_\omega \\ \dot{x}_L \end{bmatrix} = \begin{bmatrix} F_{11} & F_{12} & F_{13} & F_{14} \\ 0 & F_{22} & 0 & 0 \\ 0 & 0 & F_{33} & 0 \\ 0 & 0 & 0 & F_{44} \end{bmatrix} \begin{bmatrix} x_{rv\epsilon} \\ x_f \\ x_\omega \\ x_L \end{bmatrix} + \begin{bmatrix} w_{rv\epsilon} \\ w_f \\ w_\omega \\ w_L \end{bmatrix} \quad (9)$$

Where $x_{rv\epsilon}$ denotes a 9-dimensional navigation error state sub-vector (3 for position, 3 for velocity and 3 for orientation), x_f denotes the accelerometer error state sub-vector (b_b), x_ω denotes gyroscope error state sub-vector, x_L denotes the lever arm, $w_{rv\epsilon}$, w_f , w_ω and w_L are noises. F_{11} is standard INS navigation error matrix, and

$$F_{12} = \begin{bmatrix} 0 \\ F_{vf_b} \\ 0 \end{bmatrix}_{9 \times 3}, F_{vf_b} = R_b^n, F_{13} = \begin{bmatrix} 0 \\ 0 \\ F_{\epsilon\omega_d} \end{bmatrix}_{9 \times 3}, F_{\epsilon\omega_d} = -R_b^n,$$

$$F_{13} = \begin{bmatrix} F_{rL} \\ 0 \\ 0 \end{bmatrix}_{9 \times 3}, F_{\epsilon\omega_d} = R_b^n, F_{22} = 0_{3 \times 3},$$

$F_{33} = 0_{3 \times 3}$, F_{44} is generally zero if the GPS is fixedly mounted with respect to the IMU body; however, it can be considered as a first order Markov process if the gimbal is used for the attitude compensation of platform tilt in the aerial photogrammetric applications. It should be mentioned that if the noises w_f , w_ω are set as non-zero values, the x_f and x_ω will be modeled as random walk d_R and b_R . In this case, the whole structure of the KF will remain unchanged from the random constant model, and just with different stochastic parameter configurations.

As mentioned above, the remaining error of the scale factor can still be considered in the stochastic error model to improve the navigation performance even if it has been calibrated by the manufacturer in the factory. The scale factor error is typically considered as a random constant (Yi, 2007) or random walk (Feng, 1999). The random constant model is given here, and the state equation of the system with 12 error states of the inertial sensor of Equation (9) is modified to give Equation (10).

$$\begin{bmatrix} \dot{x}_{rv\epsilon} \\ \dot{x}_f \\ \dot{x}_\omega \\ \dot{x}_L \end{bmatrix} = \begin{bmatrix} F_{11} & F_{12} & F_{13} & F_{14} \\ 0 & F_{22} & 0 & 0 \\ 0 & 0 & F_{33} & 0 \\ 0 & 0 & 0 & F_{44} \end{bmatrix} \begin{bmatrix} x_{rv\epsilon} \\ x_f \\ x_\omega \\ x_L \end{bmatrix} + \begin{bmatrix} w_{rv\epsilon} \\ w_f \\ w_\omega \\ w_L \end{bmatrix} \quad (10)$$

where

$$F_{12} = \begin{bmatrix} 0 & 0 \\ F_{vf_b} & F_{vf_f} \\ 0 & 0 \end{bmatrix}_{9 \times 6}, F_{vf_b} = R_b^n, F_{vf_f} = \begin{bmatrix} f_1^b & 0 & 0 \\ 0 & f_2^b & 0 \\ 0 & 0 & f_3^b \end{bmatrix}$$

$$F_{13} = \begin{bmatrix} 0 & 0 \\ 0 & 0 \\ F_{\varepsilon\omega_l} & F_{\varepsilon\omega_f} \end{bmatrix}_{9 \times 6}, F_{\varepsilon\omega_l} = -R_b^n, F_{\varepsilon\omega_f} = \begin{bmatrix} (a_{fb}^b)_1 & 0 & 0 \\ 0 & (a_{fb}^b)_2 & 0 \\ 0 & 0 & (a_{fb}^b)_3 \end{bmatrix}$$

$$F_{22} = 0_{6 \times 6}, F_{33} = 0_{6 \times 6}.$$

If more items in Equations (1) and (5) are considered in the error model, the KF will perform more elegantly. If the noise in Equations (3) and (7) is zero, d_R and b_R will be same to d_b and b_b respectively. In this paper, only the d_R and d_m for the gyroscope (and b_R for accelerometer) are modeled for the stochastic error. So the error dynamic equation of the KF with 15 inertial sensor error states is given as Equation (11).

$$\begin{bmatrix} \dot{x}_{rv\varepsilon} \\ \dot{x}_f \\ \dot{x}_\omega \\ \dot{x}_L \end{bmatrix} = \begin{bmatrix} F_{11} & F_{12} & F_{13} & F_{14} \\ 0 & F_{22} & 0 & 0 \\ 0 & 0 & F_{33} & 0 \\ 0 & 0 & 0 & F_{44} \end{bmatrix} \begin{bmatrix} x_{rv\varepsilon} \\ x_f \\ x_\omega \\ x_L \end{bmatrix} + \begin{bmatrix} w_{rv\varepsilon} \\ w_f \\ w_\omega \\ w_L \end{bmatrix} \quad (11)$$

where $x_\omega = [d_R^T, d_m^T]^T$, $F_{13} = \begin{bmatrix} 0 & 0 & 0 \\ 0 & 0 & 0 \\ F_{\varepsilon\omega_l} & F_{\varepsilon\omega_m} & F_{\varepsilon\omega_f} \end{bmatrix}_{9 \times 9}$,

$$F_{\varepsilon\omega_l} = F_{\varepsilon\omega_m} = -R_b^n, F_{33} = \begin{bmatrix} 0 & 0 & 0 \\ 0 & -\frac{1}{\alpha} \cdot I_3 & 0 \\ 0 & \alpha & 0 \end{bmatrix}_{9 \times 9}, I_3 \text{ denotes}$$

the 3-order identity matrix, and other parameters are same to those in Equation (10).

3. EXPERIMENT AND ANALYSIS

In the experiment, aerial GPS/INS data was collected in September 2005 with a tactical grade IMU and dual frequency GPS receivers by the POS AV 510 system from Applanix. The gyroscope drifts in the IMU are of the order of 0.1 deg/h and the accelerometer biases are 100ug. The data rate of the IMU is 250Hz and 10Hz for the GPS. The GPS/INS integration software package Throstle™, which supports loosely-coupled and tightly-coupled models and different stochastic error models, was used to process the data with the three error models proposed in the paper. In the data processing, the loosely coupled model for the Extended Kalman Filter (EKF) is used, which is a common coupling method for the aerial GPS/INS integration because the GPS observation condition in aerial applications is much better than that in the land-based applications. Firstly the differential GPS positioning was processed with GPS high precision positioning software Caravel PP™ at a 1Hz data rate because this data rate is high enough for the GPS/INS coupling. The positioning result was compared to another GPS positioning software Graf/Nav™, and the

difference is less than 10 cm for the 200km baseline. The trajectory of the test flight is shown in Figure 1. Then the positioning result of Caravel PP was put into Throstle for the loose coupling with three stochastic models. The configurations of three tests are listed in Table 1. The data was processed also by POSpac™ to compare the result of Throstle.

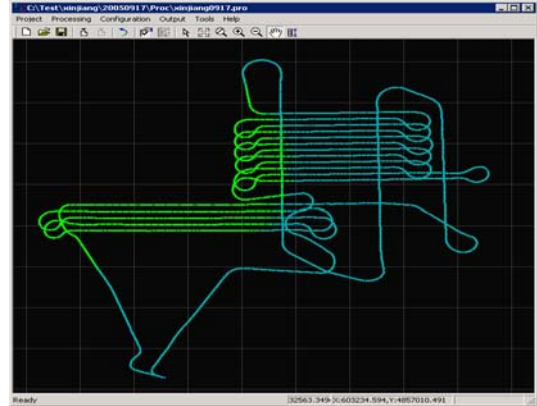


Figure 1. The trajectory of the test flight.

Items	model 1	model 2	model 3
Gyro drift random walk	√	√	√
Acce. bias random walk	√	√	√
Gyro scale factor		√	√
Acce. scale factor		√	√
Gyro drift first-order			√
Markov process			√

Table 1. The configurations of the three stochastic models.

The first test is processed with model 1 which uses 6 error states, i.e. 3 random walks for the gyroscope drifts and 3 random walks for the accelerometer biases. In order to check the performance of the KF with different stochastic models, the backward filtering and the smoothing were not implemented. The innovation (predicted residual) and measurement residual are shown in the Figures 2 and 3. The estimated errors of position (the output of the EKF) are shown in Figure 4. The estimated sensor errors are shown in Figures 5 and 6. The standard deviations of position and attitude are shown in Figures 7 and 8. The difference of the positions between the GPS differential positioning result (Caravel PP) and GPS/INS coupling result (Throstle) is shown in Figure 9. The difference of the attitude between the Throstle solution and the POSpac solution is shown in Figure 10.

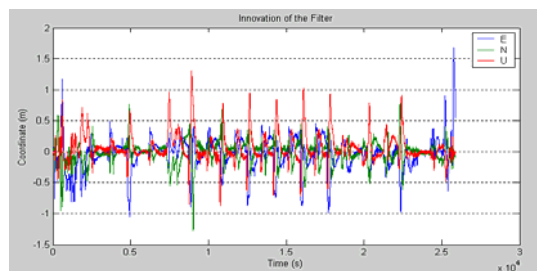


Figure 2. The innovation of the Filter with model 1.

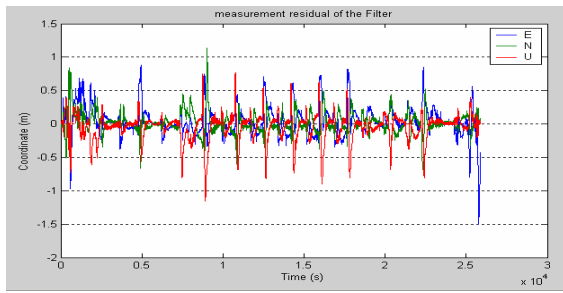


Figure 3. The measurement residual of the Filter in model 1.

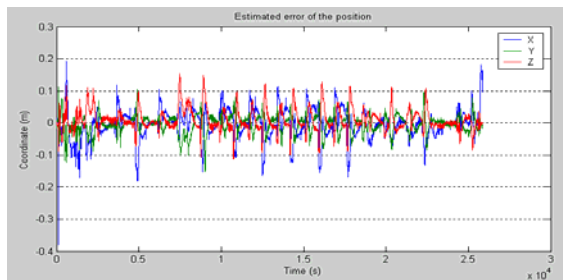


Figure 4. The estimated position error in the model 1.

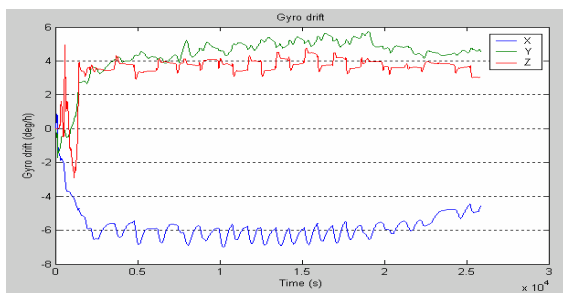


Figure 5. The estimated drift of the gyroscope in the model 1.

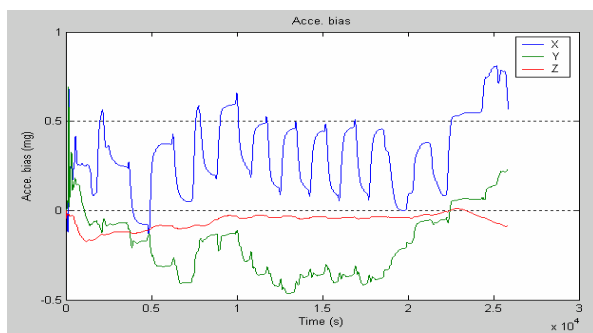


Figure 6. The estimated bias of the acce. in the model 1.

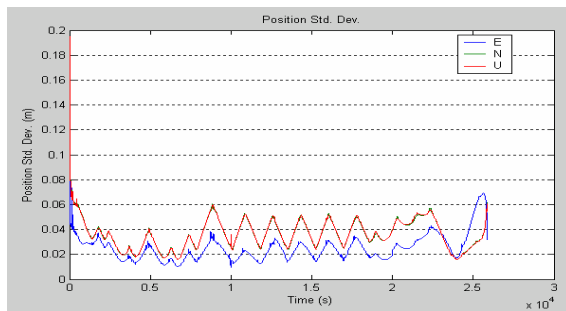


Figure 7. The Std. Dev. of position in the Filter of model 1.

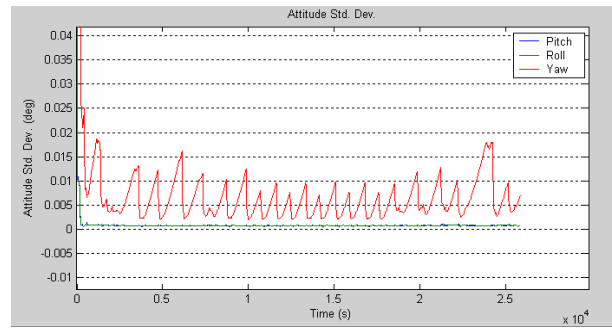


Figure 8. The Std. Dev. of attitude in the Filter of model 1.

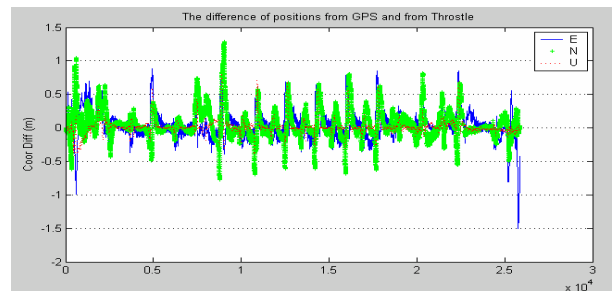


Figure 9. The position difference between the results of Throttle in the model 1 and of Caravel PP.

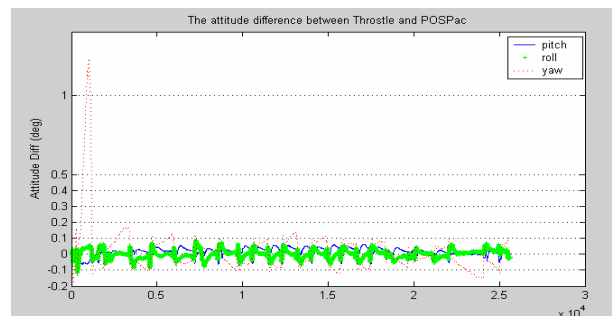


Figure 10. The attitude difference between the results of Throttle in the model 1 and of POSPac.

In Figures 2 - 10, it can be found that the predicted residual and measurement residual of the KF with model 1 are about the 0.5 - 1.0 meter. The spikes in the figures correspond to the aircraft banking where there were vehicle maneuvers. The estimated error of the position in the KF is about 10 - 20 centimeters. The estimated drifts of the gyroscopes for three axes are about 4, 5 and -6 deg/h respectively. The estimated biases of the accelerometers are 0.3, -0.3 and 0 mg for the three axes respectively, and the biases of the axes corresponding to the east and north directions vibrate intensely with the different flight strips. That means the model 1 is not good enough to describe the stochastic error in the system. The std. deviations are about 6cm for position, 4cm/s for velocity (not shown in figure), 0.002 degrees for pitch and roll, 0.01 degrees for heading. The position difference between the results of Throttle in the model 1 and of GPS is about 0.5 meter, which is consistent with the innovation of the filter. Because the GPS positioning accuracy is about 10 cm, the absolute position accuracy of the integrated system can be considered to be accurate at the 0.5-meter level. The attitude difference between the results of Throttle and of POSPac is about 0.1 degree. This result shows the 3-dimensional attitude accuracy in model 1 is at the 0.1-degree level as the attitude resolution in POS AV 510 system is

considered as 0.008 degree for heading and 0.005 degrees for the RMS of the pitch and roll. Obviously, this performance with model 1 can not reach the accuracy required for aerial photogrammetry.

The second test is processed in the model 2 with 12 error states, i.e. 3 random constants for the gyroscope drifts, 3 random constants for the accelerometer biases, 3 random constants for the gyroscope scale factors and 3 random constants for the accelerometer scale factors. The innovation and measurement residuals are shown in the Figures 11 and 12. The estimated errors of position, attitude and gyroscope drift and accelerometer bias are shown in Figures 13 - 15. The difference of the position between Caravel PP and Throstle is shown in Figure 16. The difference of the attitude between the Throstle solution and the POSPac solution is shown in Figure 17. The std. deviations are about 5m for position, 3cm/s for velocity, 0.002 degree for pitch and roll, 0.008 degree for heading.

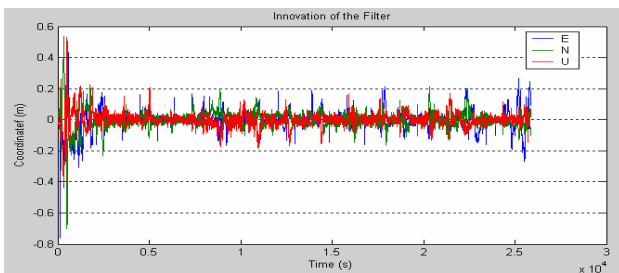


Figure 11. The innovation of the Filter with model 2.

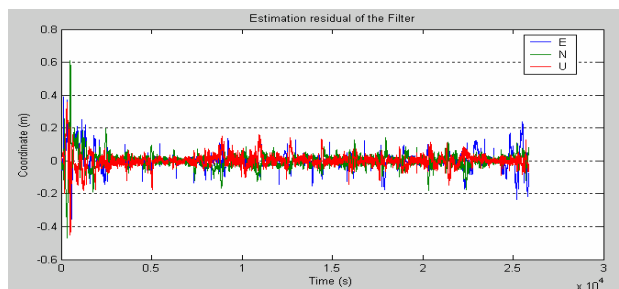


Figure 12. The measurement residual of the Filter with model 2.

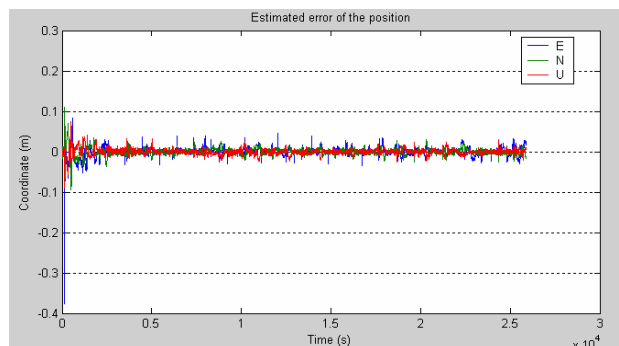


Figure 13. The estimated position error in model 2.

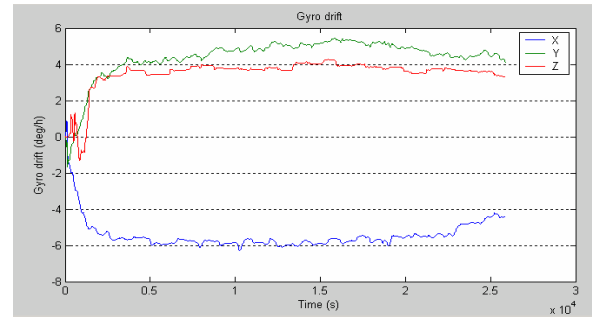


Figure 14. The estimated gyro drift in model 2.

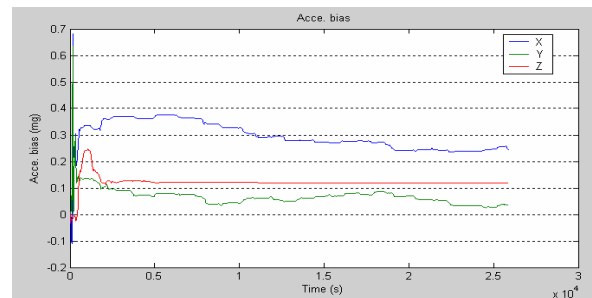


Figure 15. The estimated accelerometer bias in model 2.

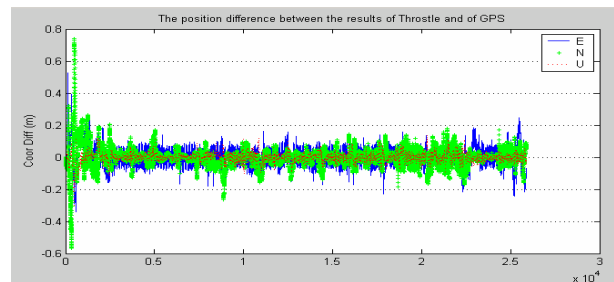


Figure 16. The position difference between the results of Throstle in model 2 and of GPS.

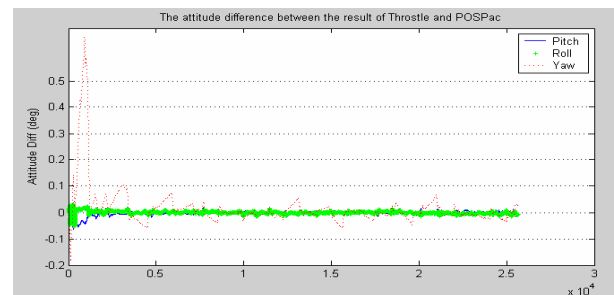


Figure 17. The attitude difference between the results of Throstlein model 2 and of GPS.

As shown in Figures 11 and 12, the predicted residual and measurement residual of the KF in model 2 are about the 0.1 - 0.2 meter, which is much better than those in model 1. The estimated error of the position in the KF is about 0.02 - 0.05 centimeters. The estimated drifts of the gyroscopes are similar to those in model 1 in general, however, they are much more stable in the short time period. The improvement is more evident for the biases of the accelerometers, where there is no

obvious correlation between the biases and the motion trajectory. The position difference between Throstle and GPS is about 0.2 meter after the stability of the filter, which indicates the absolute position accuracy in model 2 is about 0.2 meter. The differences of attitude angles are less than 0.01 degrees for both of pitch and roll, 0.05 degrees for heading. And these values can be cut down, especially for the heading, to half, i.e. 0.02~0.03 degree by smoothing or backward filtering. In this case, the Throstle can be considered as accurate as POSPac. Therefore, POSPac can not be used as a reference standard to evaluate the absolute attitude accuracy any more. Other data, e.g. the attitude from bundle adjustment or the coordinates of the ground points by traditional surveying can be used to check the final direct referencing accuracy. But these methods need the calibration of the camera boresight, which is not finished for this test data. So in this paper, these two methods are not implemented to evaluate the attitude accuracy. While the absolute accuracy specification is not achieved, from the analysis above, the result of model 2 shows obvious improvement to that of model 1.

In the 15-state error model a Markov process in the gyroscope drift is added to model 2. The std. deviations for position, velocity and attitude are almost the same as those in Model 2. In this section, the attention is paid to the gyro drift and accelerometer bias as shown in Figures 18 and 19, and the difference of position (and attitude) between Throstle and GPS (POSPac) is shown in Figure 20 and 21. By comparing the Figures 18 - 21 and Figures 14 - 17, it can be found the differences are not obvious, which means the improvement of the 15-state error model relative to the 12-state error model is limited. This is probably due to the limited observation capability of the gyroscope data or the unsuitable configuration of the stochastic model parameters. The testing and analysis are ongoing efforts for which more detailed analysis and results will be provided later.

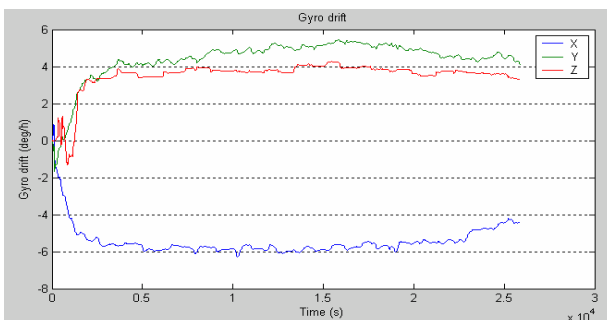


Figure 18. The estimated gyro drift in model 3.

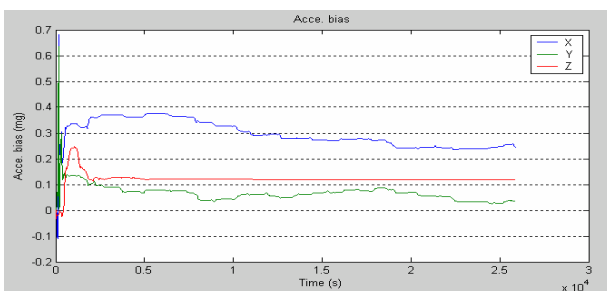


Figure 19. The estimated accelerometer bias in model 3.

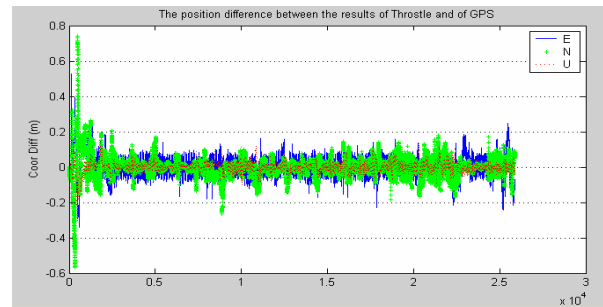


Figure 20. The position difference between the results of Throstle in model 3 and of GPS.

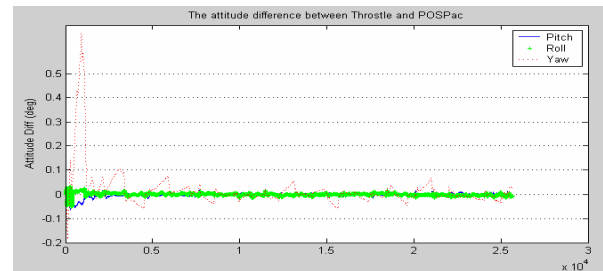


Figure 21. The attitude difference between the results of Throstlein model 3 and of GPS.

4. CONCLUSIONS

In this paper, the 6-state, 12-state and 15-state inertial sensor error models are implemented, and the KF performance of each is compared and analyzed. The accuracies of the integrated system reach 5cm for position, 3cm/s for velocity, 0.002 degree for pitch and roll, 0.008 degree for heading in the 12-state model, which are all better than those in the 6-state error model. However, the improvement of the 15-state error model from 12-state error model is limited and insignificant. Further investigation is going for the absolute accuracy validation of the GPS/INS integration based on different models. And more precise stochastic error model will also be tested.

ACKNOWLEDGEMENTS

This research is supported by the Chinese National Scientific Foundation (No. 40501060). The test flight discussed here is supported by the Xinjiang Surveying and mapping Bureau. The support of these agencies is gratefully acknowledged.

REFERENCES

- Abdullah, Q., 1997, Evaluation of GPS-Inertial Navigation System for airborne photogrammetry: *ASPRS/MAPPS Softcopy Conference*, Arlington, 1997.
- Feng S., 1999. *Research on the low cost IMU/GPS integrated navigation system*. Ph.D. Dissertation. Najing University of Aeronautics and Astronautics. 1999.
- Grejner-Brzezinska D. A., 1999. Direct Exterior Orientation of Airborne Imagery with GPS/INS System: Performance Analysis, *Navigation*, Vol. 46, No. 4, pp. 261-270.

- Grejner-Brzezinska D. A., 2001. Direct sensor Orientation of Airborne and Land-based Mapping Applications, Report No. 461, Geodetic GeoInformation Science, Department of Civil and Environmental Engineering and Geodetic Science, The Ohio State University.
- Grejner-Brzezinska D. A., Toth C., and Yi Y., 2005. On Improving Navigation Accuracy of GPS/INS Systems, *Photogrammetric Engineering & Remote Sensing*, Vol. 71, No. 4, pp.377-389.
- Mostafa, M.M.R., Hutton J., and Lithopoulos E., 2001. Direct Georeferencing of Frame Imagery: An Error Budget, *Proceedings of The Third International Mobile Mapping Symposium*, Cairo, Egypt, January 3-5.
- Cramer M., Stallmann D. and Haala N., 2000. Direct Georeferencing Using GPS/Inertial Exterior Orientations For Photogrammetric Applications, *IAPRS*, Vol. XXXIII, Amsterdam, 2000.
- Cramer M., 2001. Performance of GPS/Inertial Solutions in Photogrammetry, *Photogrammetrische Woche 2001*, Fritsch/Spiller (Eds.)
- IEEE Std 1293, 1998. IEEE Standard Specification Format Guide and Test Procedure for Linear, Single-Axis, Nongyroscopic Accelerometers, The Institute of Electrical and Electronics Engineers, Inc., New York, NY.
- IEEE Std 952, 1999. IEEE Standard Specification Format Guide and Test Procedure for Single-Axis Interferometric Fiber Optic Gyros, Institute of Electrical and Electronics Engineers, Inc., New York, NY.
- IEEE Std 528, 2001. IEEE Standard for Inertial Sensor terminology, published by The Institute of Electrical and Electronics Engineers, Inc., New York, NY.
- Scaloud J., Cramer M., Schwarz K. P., 1996. Exterior Orientation by Direct Measurement of Camera Position and Attitude, *International Archives of Photogrammetry and Remote Sensing*, Vol. XXXI, Part B3, pp. 125-130.
- Schwarz K. P., Wei M., Gelderen M., 1994. Aided versus embedded-a comparison of two approaches to GPS/INS integration. *Proceedings of IEEE PLANS 94*, pp. 314-322.
- Toth C., Grejner-Brzezinska D. A., 1998. Performance Analysis Of The Airborne Integrated Mapping System (AIMS™), *ISPRS Commission II Symposium on Data Integration: Systems and Techniques*, July 13-17, Cambridge, England, pp.320-326.
- Yi Y., (2007). *On Improving the Accuracy and Reliability of GPS/INS-based Direct Sensor Georeferencing*. Ph.D. Dissertation. The Ohio State University. 2007.

